

Article

The Effects of Load on Transmural Differences in Contraction of Isolated Mouse Ventricular Cardiomyocytes

Running title: Load Effects on Transmural Differences in Mechanics of Cardiomyocytes

Anastasia Khokhlova ^{1,2,*}, Gentaro Iribe ³, Leonid Katsnelson ^{1,2}, Keiji Naruse ³
and Olga Solovyova ^{1,2}

¹ Ural Federal University, Mira 19, Ekaterinburg 620002, Russia;

l.katsnelson@iip.uran.r (L.K.); soloveva.olga@urfu.ru (O.S.)

² Institute of Immunology and Physiology, Russian Academy of Sciences, Pervomajskaya 106, Ekaterinburg 620049, Russia

³ Dentistry and Pharmaceutical Sciences, Graduate School of Medicine, Okayama University, Shikata cho 2-5-1, Okayama 1700-8558, Japan; iribe@okayama-u.ac.jp (G.I.);

knaruse@md.okayama-u.ac.jp (K.N.)

* Correspondence: a.khokhlova@iip.uran.ru or a.d.khokhlova@urfu.ru

ABSTRACT

Mechanical properties of cardiomyocytes from different transmural regions are heterogeneous in the left ventricular wall. The cardiomyocyte mechanical environment affects this heterogeneity because of mechano-electric feedback mechanisms. In the present study, we investigated the effects of load upon transmural differences in contraction of subendocardial (ENDO) and subepicardial (EPI) single cells isolated from the murine left ventricle. Various loads were applied to the cells using carbon fiber techniques for single myocytes. To simulate experimentally obtained results and to predict mechanisms underlying the cellular response to change in load, our mathematical models of the ENDO and EPI cells were used. Extent of the transmural gradient in the time course of contractions was independent of the loading conditions where unloaded and heavy loaded (isometric) contractions were examined, but the regional gradient of the relaxation time characteristics tended to decrease when the load decreased. Under auxotonic contractions, time to peak contraction (T_{max}) was significantly longer in ENDO cells than in EPI cells at low preload. An increase in preload (axial stretch) prolonged T_{max} in both cell types; however, the prolongation was greater in EPI cells, resulting in a decrease in transmural gradient in T_{max} at high preload. The $[Ca^{2+}]_i$ transient decay time constant was consistent with the greater preload dependency in T_{max} of EPI cells. Our modified mathematical models reproduced experimental results, suggesting that differences in cooperativity of cross bridges and calcium troponin C complex interactions between the ENDO and EPI cardiomyocytes may contribute to

the different cellular responses to stretch, which may provide a decrease in transmural dispersion of cellular shortening in the intact heart.

Highlights

- Mechanical behavior of ENDO and EPI cells was examined at different loads
- ENDO and EPI cells were different in their mechanical response to changes in preload
- Underlying subcellular mechanisms are predicted via mathematical cellular models

Keywords: ventricular transmural heterogeneity; cellular mechanics; load dependency; calcium transient; mechano-calcium feedback

1. INTRODUCTION

The heterogeneity in electrophysiological properties of the myocardium has been investigated. Experiments on isolated ventricular cardiomyocytes or wedges from ventricular wall have shown that the action potential (AP) duration is longer in the inner subendocardial (ENDO) region than in the outer subepicardial (EPI) and midmyocardial (MID) regions in mice, rats, guinea pigs, dogs, and humans [1-6]. This transmural heterogeneity in AP morphology and duration is attributed to the differences in ion channel expression [2, 7, 8]. However, Taggart and co-workers found that regional AP duration gradients in the whole heart are not as pronounced as that in isolated cells, possibly because of the electrotonic coupling of cardiomyocytes across the ventricular wall [9].

Studies on the transmural gradient in the mechanical properties and the consequences of mechano-electric feedback on regional differences in electrophysiological function in the healthy heart and under pathological conditions are just beginning. Several studies showed that ENDO and EPI cardiomyocytes from the ventricular wall differ in their mechanical properties. ENDO cells demonstrate greater shortening with slower time to peak shortening and delayed relaxation of contraction compared with EPI cells in guinea pig and canine hearts under mechanically unloaded shortening [3, 4]. Recently, Ashikaga and co-workers showed that in the whole dog heart, *in vivo* transmural gradients in ventricular wall stress and strain also exist [10]. Data observed with high-resolution tissue Doppler imaging showed asynchronous deformation of ENDO and EPI layers during isovolumic contractions [11]. However, cellular and subcellular mechanisms of this heterogeneity remain unclear.

Cazorla and co-workers showed that the sarcomere length (SL)–tension relationship is different between the ENDO and EPI single cells isolated from rat, ferret, and guinea pig healthy ventricles [12, 13]. They showed that the slope of the SL–active auxotonic tension relationship is

steeper in ENDO than in EPI cardiomyocytes. Similar studies were recently performed using ENDO and EPI cells from the right and left ventricles of the guinea pig [14]. However, they found no significant difference in the slope of the cell length–auxotonic tension curves between ENDO and EPI cardiomyocytes.

In the present study, we investigated the mechanical response of cardiomyocytes isolated from ENDO and EPI regions of mouse left ventricle (LV) to changes in the mechanical load using our recently developed single cell stretch method [15]. To clarify transmural differences in excitation–contraction coupling at various preloads, we examined regional differences in cellular $[Ca^{2+}]_i$ transient. To predict subcellular mechanisms responsible for the differences, we used our mathematical ENDO and EPI cellular models, which accounts for the transmural gradients between the cells in calcium handling and myofilament contractile mechanisms.

2. MATERIALS AND METHODS

2.1. Myocyte Preparation

We conducted all experiments in accordance with the Guiding Principles for the Care and Use of Animals approved by the Council of the Physiological Society of Japan, and the study protocol was approved by the Animal Subjects Committee of Okayama University Graduate School of Medicine, Dentistry and Pharmaceutical Sciences.

Left ventricular myocytes were enzymatically isolated from 22 hearts excised from male C57B/6 mice (8–10 weeks of age), which were sacrificed by overdose with isoflurane (DS Pharma Animal Health, Osaka, Japan). Hearts were swiftly cannulated via the aorta for perfusion conducted at 37°C with a sequence of two solutions (in mM): (1) oxygenated Ca^{2+} -free solution containing NaCl (128), KCl (2.6), $MgSO_4$ (1.18), KH_2PO_4 (1.18), Hepes (10), taurine (20), and glucose (11) (pH adjusted to 7.4 using NaOH) supplemented with 10 mM 2,3-butanedione monoxime (BDM) (Sigma-Aldrich, St. Louis, MO, USA) and perfused for 1–2 minutes at a rate of 4 ml/min and then for 3–4 minutes at a rate of 3 ml/min; and (2) oxygenated Ca^{2+} -free solution 1 supplemented with 10 mM BDM (Sigma-Aldrich, St. Louis, MO, USA), enzyme Liberase™ Research Grade (0.093 mg/ml; Roche, Basel, Switzerland) 12.5 μ M $CaCl_2$, and perfused for 6–7 minutes at a rate of 3 ml/min.

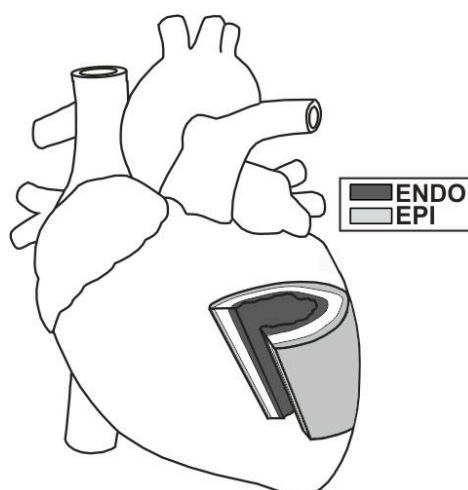


Figure 1. The isolation protocol. Cardiomyocytes from ENDO and EPI regions of the central LV region were collected. Basal and apical regions were excluded.

Each heart was dissected and several strips (approximately 0.1 mm×0.2 mm) were collected from subendocardium and subepicardium of the central region of the LV with basal and apical regions being excluded (Fig. 1). Further incubation of tissue strips at 37°C with enzyme solution 2 resulted in the isolation of separate populations of ENDO and EPI cardiomyocytes. The cells were collected in separate tubes containing solution 1 supplemented with 12.5 μM CaCl_2 and 10% fetal bovine serum (FBS; Sigma-Aldrich, USA) and then centrifuged for 3 minutes at 15×g (Kusota, Tokyo, Japan) using a soft-start/soft-stop protocol.

After centrifugation, the supernatant was discarded and the cell pellet was carefully resuspended in Ca^{2+} -free solution 1 containing 600 μM CaCl_2 . The centrifugation step was repeated twice. The final pellet was resuspended in solution 1 containing 1.8 mM CaCl_2 . Isolated myocytes were stored in Tyrode solution containing (in mM): NaCl (140), KCl (5.4), CaCl_2 (1.8), MgCl_2 (1.0), Hepes (5), and glucose (11) (pH adjusted to 7.4 using NaOH) at room temperature (22–24°C). The cardiomyocytes selected for study showed clear sarcomere patterns and were quiescent when not stimulated. All experiments were performed at a stimulation frequency of 1 Hz at room temperature.

2.2. Measurements of $[\text{Ca}^{2+}]_i$

For measurement of $[\text{Ca}^{2+}]_i$ ENDO and EPI cardiomyocytes were loaded with the membrane-permeable acetoxymethyl ester form of Fura-4F (Fura-4F AM; Thermo Fisher Scientific, Waltham, MA, USA). Cells were loaded with 2.5 μM Fura-4F AM by incubating them in NT solution containing 0.1% Pluronic[®] F-127 (AnaSpec, Fremont, CA, USA) for 10 minutes at room temperature.

Fura-4F AM loaded myocytes were placed in an experimental chamber, and alternately excited at 250 Hz with 340 and 380 nm light. The emitted fluorescence was collected at 480–520 nm using a photomultiplier tube (IonOptix Corporation, Milton, MA, USA). The ratio of the fluorescence intensity excited with 340 and 380 nm wavelength light (F_{340}/F_{380}) was calculated after subtracting the background fluorescence, and this was used as an index of change in $[Ca^{2+}]_i$ to compare the relative diastolic levels, amplitudes, and the time course of $[Ca^{2+}]_i$ between ENDO and EPI myocytes.

Time to peak of $[Ca^{2+}]_i$ was measured from the onset to the peak of the F_{340}/F_{380} ratio. The decay of the F_{340}/F_{380} ratio (from peak to 100% of the decline phase) was fit to a single exponential function whose time constant, τ , was used to evaluate $[Ca^{2+}]_i$ decay.

2.3. The single myocyte stretch system and measurement of cellular mechanical activity

The single myocyte stretch system has been described in detail elsewhere [15]. Briefly, each cell end was held to the top and bottom surfaces of the cell by a pair of carbon fibers (CFs) to set different loading conditions (unloaded, uncontrolled auxotonic, and heavy loaded (isometric) twitches were achieved) or to apply various extents of preload (axial stretch) to the cells. Each CF on the left side was mounted on a computer-controlled piezoelectric transducer (PZT). Both CFs received the same control command to achieve identical CF position control for stretching the cell end in one direction.

2.4. Length and force measurements

The detailed method for performing length and force measurements is described elsewhere [16]. Briefly, cell length signal (CF tip distance) and SL changes were recorded using the IonOptix equipment and software (IonOptix Corporation, Milton, MA, USA). Active and passive forces were calculated as follows: $F = K \cdot (\Delta L_{CF} - \Delta L_{PZT})$, where K is the combined stiffness of the left CFs, ΔL_{CF} is the change in distance between left and right CFs, and ΔL_{PZT} is the change in PZT position.

Tension of the cell was calculated as the force normalized to the effective cross-sectional area. Effective cell cross-sectional area was calculated from the measured cell width, assuming an elliptical shape of the cross section with a 3:1 ratio of long (measured cell width, y -direction) and short axes (estimated cell height, z -direction) [16].

Figure 2 shows representative auxotonic contractions under the mechanical load of the carbon fibers from a range of preloads (end-diastolic sarcomere length (SL_0) changes from approximately 1.76–1.82 μm) and calculated tensions superimposed for various preloads.

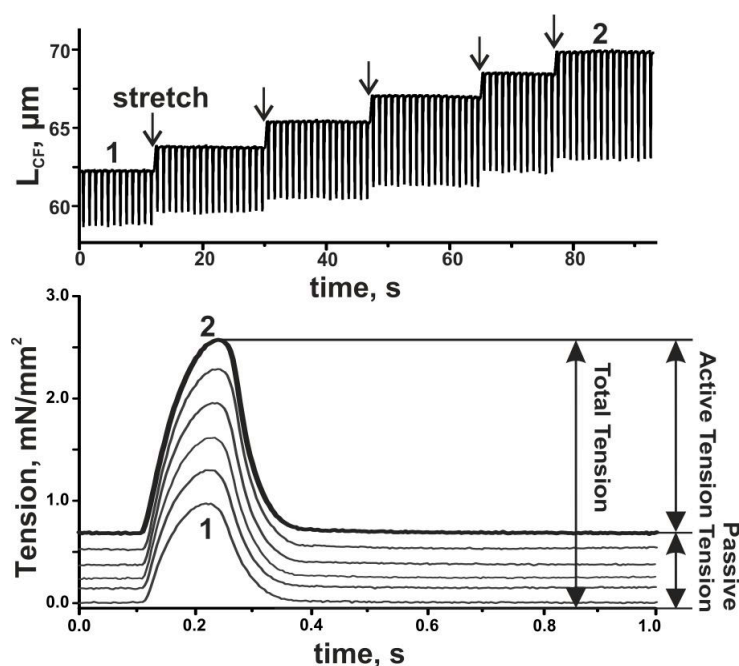


Figure 2. Representative auxotonic contractions of the mouse ventricular cardiomyocyte recorded at various preloads. Top panel: representative experimental record of cardiomyocyte shortening during auxotonic twitches at various preloads where L_{CF} is the distance between left and right CFs. Bottom panel: cellular tension recordings superimposed for various preloads detailing separate twitches from the top panel. Arrows show the stretch applied.

The slopes of end-diastolic force length relation curve (EDFLR) and the end-systolic force length relation curve (ESFLR) were used as indices of myocardial stiffness and cardiac contractility, respectively. EDFLR and ESFLR were fitted by a linear regression line of total and passive amplitudes for auxotonic twitches at various preloads (Fig. 3). Iribe and co-workers reported that within a sarcomere length range approximately less than $2.0 \mu\text{m}$, ESFLR is unaffected by loading conditions in single ventricular guinea pig cardiomyocytes [16]. To simplify the identification of EDFLR and ESFLR, preload was kept within this range.

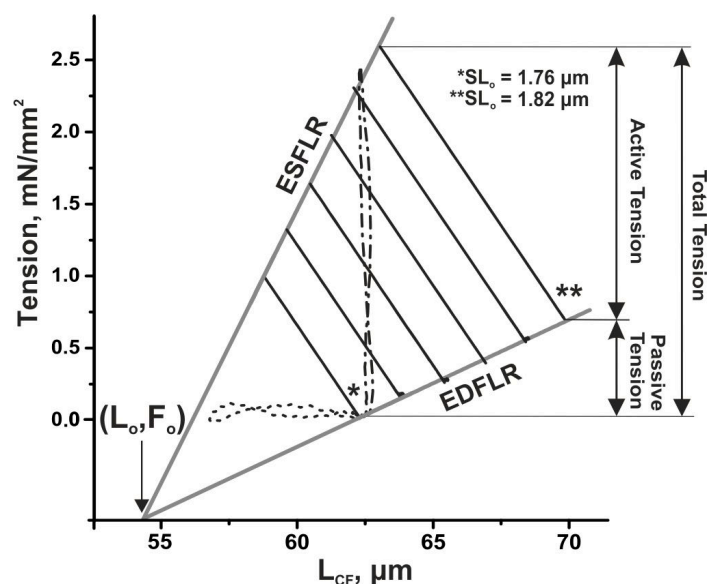


Figure 3. Force-Length (FL) relationship curves in single cardiomyocytes. Solid black lines show FL relationships between auxotonic contractions at various preloads from approximately 1.76–1.82 μm and end-diastolic sarcomere length (SL_o). The dotted line and dashed lines show FL relationships between the unloaded and heavy loaded (isometric) contractions, respectively, obtained at an approximate SL_o of 1.76 μm . Grey solid lines show the end-diastolic FL relation curve (EDFLR) and end-systolic FL relation curve (ESFLR). (L_o, F_o) , intersection point of EDFLR and ESFLR.

2.5. Loading condition control

The detailed method for adaptive feed-forward control to apply different loading conditions to the cell has been described elsewhere [16]. Briefly, the length signal in steady state auxotonic contractions was recorded and averaged for 10 beats, and was then used as the source signal for a PZT command. For isometric contractions (heavy loaded), an appropriately amplified source signal was inverted and applied to make outward PZT movement compensate for the cell shortening. For unloaded contractions, an appropriately amplified source signal was applied to make inward PZT movement prevent changes in CF bending [16].

2.6. Contraction profile and instantaneous elastance curve

To compare the time-dependent profile of contractions between the cell types at various preloads, we used the following temporal characteristics: the time to peak (T_{max}) and the time to 50% relaxation (TR_{50}) of auxotonic contractions measured as the time interval from T_{max} to the time of 50% relaxation.

To compare the time-dependent profiles of cellular contraction under different loading conditions, we used the instantaneous elastance approach proposed by Suga and co-workers in

their study on the whole heart [17]. According to this approach, the instantaneous elastance (or reciprocal compliance) of the cell is defined as the time-varying ratio of instantaneous force $F(t)$ to instantaneous length $L(t)$: $E(t) = (F(t) - F_o)/(L(t) - L_o)$, where L_o and F_o are the length and force values at the intersection of ESFLR and EDFLR, respectively (Fig. 3, [16]). The elastance reflects the change in the amount of tension produced for the length unit and allows comparison of temporal properties of force generation in the cell under different loading conditions. Here, we used the time to peak of elastance curve (ET_{max}) and the time to 50% relaxation (ETR_{50}) as the time-dependent characteristics of the $E(t)$ profile.

2.7. Statistics

All values are presented as the mean \pm standard error of the mean (SEM). A Student's unpaired t -test and a two-way ANOVA with Bonferroni post-test were used for statistical analysis, and a p value of <0.05 was considered to indicate a significant difference between means.

2.8. Mathematical models

To predict mechanisms responsible for the transmural differences in mechanical properties of cardiomyocytes, we used our mathematical models of ENDO and EPI cells [18]. Our EPI and ENDO models have been developed based on experimental data and they mimic regional differences in calcium handling and cellular contractile function in ventricular cardiomyocytes. The complete set of equations and parameters for each of the cell type models are provided elsewhere [18]. To reproduce species-specific features of the amplitude and time course of contractions in mouse ventricular cardiomyocytes, we modified parameters for mechanical variables of the models (Table 1). We describe here the main equations of the model mechanical block and specific parameters for the mouse EPI and ENDO models used in this study.

Passive tension is described as follows:

$$F_{passive} = \beta_2 \cdot (e^{\alpha_2 \cdot l(t)} - 1), \quad (1)$$

where $l(t)$ is deformation of the cell against its slack length per sarcomere, and β_2, α_2 is the scaling parameter fitted for the mouse contraction (Table 1).

Active tension of the cell is defined by the amount of force-generating cross-bridges (Xbs), which depends on the velocity of sarcomere shortening/lengthening:

$$F_{CE} = \lambda \cdot N \cdot p(v), \quad (2)$$

where λ is the scaling parameter fitted for the mouse contraction (Table 1), N is the fraction of Xbs [Xb]. Function $p(v)$ describes the dependence of the average Xb force on the sarcomere

shortening/lengthening velocity $v(t) = \dot{l}_1(t)$, where $l_1(t)$ is the deformation of the sarcomere against its slack length.

$N(t)$ depends on the sarcomere mechanics that assures a key molecular mechanism of the mechano-calcium-electric feedback in cardiomyocytes in the framework of our models [18]:

$$\frac{dN}{dt} = k_{pv} \cdot M([CaTnC]) \cdot n_1(l_1) \cdot L_{oz}(l_1) \cdot (1 - N) - k_{mv} \cdot N, \quad (3)$$

where k_{pv} and k_{mv} are the velocity-dependent rate constants of Xb attachment and detachment, respectively, $n_1(l_1)$ is the probability of a myosin head “finding” a vacant site on the actin filament, and $L_{oz}(l_1)$ is the normalized linear dependence of the sarcomere overlap zone on the SL.

Xb kinetics is affected by kinetics of CaTnC complexes. In the models, we took into account cooperative end-to-end interaction between adjacent tropomyosins on the thin filament (*RU end-to-end cooperativity*). We suggest that Ca^{2+} binding by TnC, located between neighboring regulatory units (RUs) of the thin filament, induces end-to-end interactions between adjacent tropomyosins, thus allowing opening of the additional actin sites for myosin head attachment [19]. In Eq. (4), $M[CaTnC]$ indicates the RU end-to-end cooperativity:

$$M([CaTnC]) = \frac{([CaTnC])^{\mu \cdot (1+0.6\mu)}}{([TnC]_{tot})^{\mu+0.6\mu}}, \quad (4)$$

where $[CaTnC]$ is the concentration of CaTnC complexes, $[CaTnC]_{tot}$ is the total TnC concentration, and μ is the RU cooperativity factor (Table 1). Recently, we showed that difference in μ between the ENDO and EPI models contributes to the regional differences in active force amplitude in the models [20]. Specific values of fitted μ for the ENDO and EPI models of mouse cardiomyocytes are shown in Table 1.

A key feature of our models is the cooperative mechanisms of myofilament Ca^{2+} activation. Two cooperative mechanisms are accounted for in the equation for the CaTnC kinetics:

$$\frac{d[CaTnC]}{dt} = k_{on} \cdot ([TnC]_{tot} - [CaTnC]) \cdot [Ca^{2+}]_i - k_{off} \cdot e^{-k_A} [CaTnC] \cdot \pi_{N_A} \cdot [CaTnC], \quad (5)$$

where k_{on} and k_{off} are the rate constants of CaTnC binding and dissociation, respectively.

Here, we briefly describe the formulae were previously developed [19, 21] for these types of cooperativity:

Xb-CaTnC cooperativity: the rate of CaTnC dissociation decreases with an increase in [Xb] per single CaTnC complex.

The dependence π_{N_A} expressing this cooperativity in the Eq. (5) may be written as follows:

$$\pi_{N_A} = \pi_{min}^{f_A \cdot N_A} \quad (6)$$

where π_{min} is the model parameter, f_A is the Xb-CaTnC cooperativity factor, and N_A means an average [Xb] falling on one CaTnC complex, as follows:

$$N_A = N \frac{[TnC]_{tot}}{[CaTnC]} \quad (7)$$

CaTnC-CaTnC cooperativity: the rate of CaTnC complex dissociation decreases with increasing numbers of CaTnC complexes in the proximity.

Dependence $e^{-k_A[CaTnC]}$ defines this cooperativity in Eq. (5), where k_A is the CaTnC-CaTnC cooperativity factor.

The reference values of k_{off} , f_A , and k_A for the ENDO and EPI models are shown in Table 1. Additionally, we varied these parameters to evaluate their role in the preload dependency in contraction of ENDO and EPI cells. Below, we used four EPI models (reference, decreased k_{off} ($\downarrow k_{off}$), increased CaTnC-CaTnC cooperativity (\uparrow CaTnC-CaTnC coop), and increased Xb-CaTnC cooperativity (\uparrow Xb-CaTnC coop); see Table 1).

Table 1. Parameters for the main mechanical variables of ENDO and EPI models

Model parameters	Definition	ENDO	EPI (reference)	EPI ($\downarrow k_{off}$)	EPI (\uparrow CaTnC-CaTnC coop)	EPI (\uparrow Xb-CaTnC coop)	Source
α_2 [μm^{-1}]	elasticity constant scaling	10	10	10	10	10	Eq. (1)
β_2 [mN mm^{-2}]	coefficient for passive tension scaling	0.11	0.1	0.1	0.1	0.1	Eq. (1)
λ [mN mm^{-2}]	coefficient for sarcomere ensemble force	10	10	10	10	10	Eq. (2)
μ	RU end-to-end cooperativity factor	2.5	3.6	3.6	3.6	3.6	Eq. (4)
k_{off} [s^{-1}]	rate constant of CaTnC dissociation	200	200	155	200	200	Eq. (5)
k_A [mM^{-1}]	CaTnC-CaTnC cooperativity factor	22	22	22	33	22	Eq. (5)
f_A	Xb-CaTnC cooperativity factor	0.75	0.75	0.75	0.75	1.1	Eq. (7)

Other parameters for the ENDO and EPI(reference) models are provided elsewhere [18].

3. RESULTS

3.1. The effects of preload on transmural gradient in contraction and excitation–contraction coupling

No significant difference in slack SL_o was found between the ENDO and EPI cells ($p=0.91$, ENDO $1.761\pm 0.012\ \mu\text{m}$ ($n=25$); EPI $1.756\pm 0.020\ \mu\text{m}$ ($n=24$)). To examine transmural differences in ENDO and EPI cardiomyocytes in response to changes in preload, single myocytes were stretched (Fig. 1) from their slack SL_o (control) through several steps under auxotonic contractions. An average increase in SL_o was about 3.5% (ENDO $3.43\pm 0.24\%$; EPI $3.55\pm 0.28\%$; stretch). Figure 4 shows representative recordings of auxotonic contractions of ENDO and EPI isolated cardiomyocytes at low preload (control) and high preload (stretch).

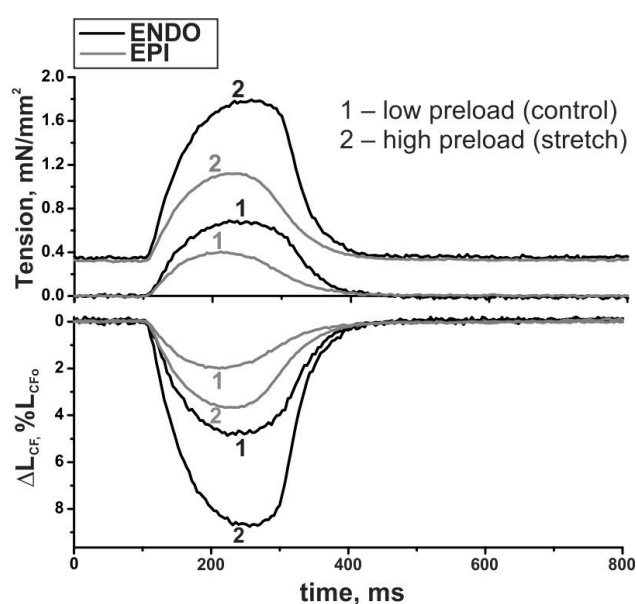


Figure 4. Representative recordings of auxotonic twitch force (top panel) and cell length (bottom panel) of ENDO and EPI isolated cardiomyocytes from the same heart recorded at various preloads. L_{CF0} is the end-diastolic distance between left and right CFs.

3.1.1. Regional differences in the time course of contraction

In auxotonic contractions, ENDO cells showed significantly longer time to peak contraction (T_{max}) compared with EPI cells at slack SL_o ($p<0.01$, Fig. 5). Axial stretch prolonged T_{max} in both groups ($p<0.01$, Fig. 5). However, EPI cells showed significantly greater prolongation of the T_{max} compared to ENDO cells (interaction between the groups $p<0.05$), resulting in a decrease in transmural gradient in T_{max} in the stretched state. Relative differences in mean T_{max} of EPI compared with ENDO cells decreased from 17% in control to 13% at stretch (Fig. 5, left panel). In contrast, time to 50% relaxation (TR_{50}) was not significantly different between the groups at slack SL_o and did not change in the stretched state ($p=0.5$, control: ENDO

67.68±3.34 ms (25), EPI 65.63±3.15 ms (24); stretch: ENDO 63.12±2.81 ms (25), 63.83±2.83 ms (24)).

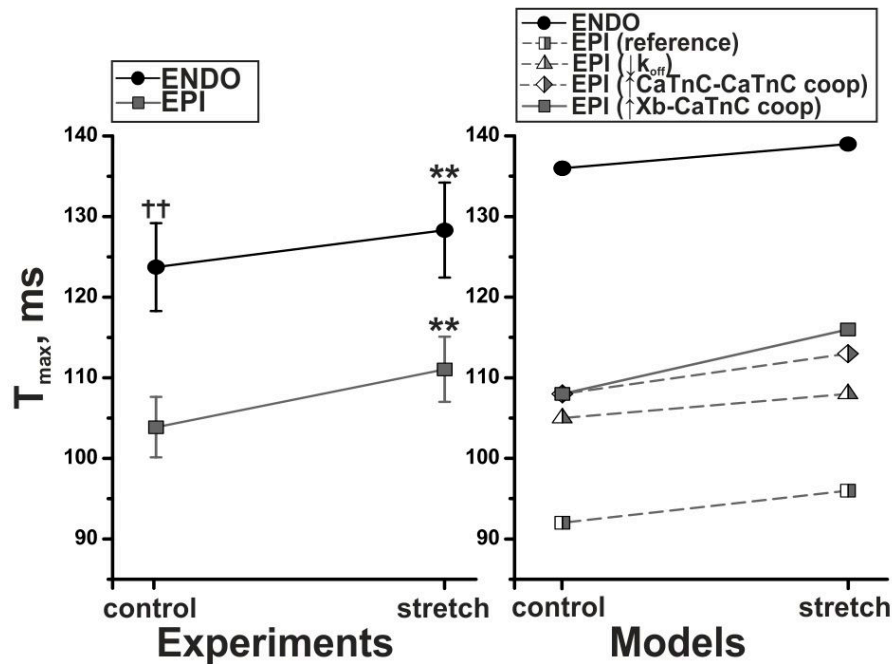


Figure 5. Transmural gradient in the time to peak contraction (T_{max}) between single ENDO and EPI cells at various preloads in wet experiments (ENDO: $n=25$, EPI: $n=24$) and mathematical models. ** Control vs. stretch, $p<0.01$; †† ENDO vs. EPI, $p<0.01$

Our ENDO and reference EPI mathematical models reproduce experimental findings on prolongation of T_{max} with increasing preload in each cell type (Fig. 4, right panel). Previously, we analyzed the mechanisms underlying the preload dependency in T_{max} in our models [21, 22]. Here, we briefly illustrate the mechanisms (Fig. 6). Stretch leads to a decrease in the distance between actin and myosin filaments as a consequence of spatial rearrangement in a constant cytosolic volume. This, together with an increase in filament overlap, increases $[Xb]$ that, because of the Xb-CaTnC cooperativity mechanisms, causes an increase in TnC affinity for Ca^{2+} . This, together with CaTnC-CaTnC cooperativity mechanism, leads to a subsequent slowing down of the CaTnC dissociation that delays a decrease in $[Xb]$. Thus, stretch causes prolongation of the T_{max} (Fig. 6).

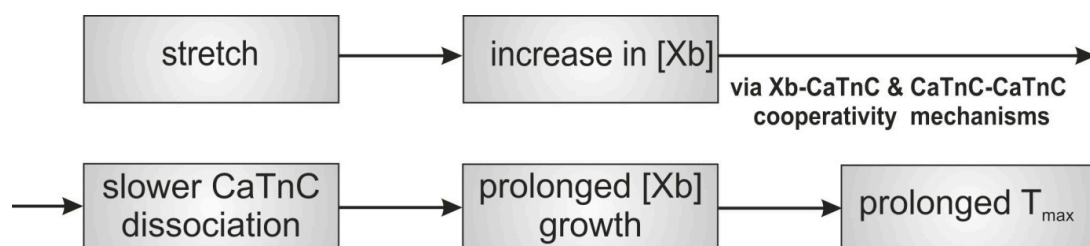


Figure 6. Model mechanisms of stretch effect on time to peak contraction (T_{max}).

Despite qualitative agreement between model predictions and experimental findings on an increase in T_{\max} in both cell types, our ENDO and reference EPI models failed to reproduce a decrease in the transmural T_{\max} gradient at a high preload, because the relative difference between the mean ENDO and EPI T_{\max} (with respect to the ENDO value) did not change in the models in the stretch versus control states (32% vs. 31%, respectively, Fig. 5, right panel). Moreover, ENDO and reference EPI models quantitatively produced much higher regional differences in T_{\max} under either control or stretch conditions compared with experimental data. To correct these mismatches, we used the models to test the hypothesis that there is a steeper slowing down of CaTnC dissociation at higher preload in the EPI cells, which may contribute to a steeper preload dependency in T_{\max} in the EPI cells (Fig. 6). We tested several model hypotheses on a potentially steeper slowing down of CaTnC dissociation in the EPI cells, as follows: (i) a decrease in the CaTnC dissociation rate constant; (ii) an increase in CaTnC-CaTnC cooperativity; and (iii) an increase in Xb-CaTnC cooperativity (see Fig. 4, right panel, EPI (\downarrow koff), EPI (\uparrow CaTnC-CaTnC coop), and EPI (\uparrow Xb-CaTnC coop), respectively; model parameters are shown in Table 1). The first two hypotheses (i.e. (i) and (ii)) for the EPI model did not change the slope of preload dependency in T_{\max} , while an increase in Xb-CaTnC cooperativity in the EPI model (i.e., (iii)) resulted in an increase in T_{\max} under the control and stretched states, and increased the steepness of the preload dependency for T_{\max} in the EPI model compared with the ENDO model (Fig. 5, right panel). Thus, a higher degree of Xb-CaTnC cooperativity in the EPI model allowed us to reproduce our experimental findings more adequately both quantitatively and qualitatively, because the relative differences between the ENDO and EPI models in the mean T_{\max} were 21% for control and 16% for the stretched state, which were closer to experimental values. The transmural difference in T_{\max} also decreased when preload increased (Fig. 5, right panel, ENDO vs. EPI (\uparrow Xb-CaTnC coop)).

Thus, modeling results suggest that specific features of length-dependent cooperativity in myofilament activation by Ca^{2+} accounted for the ENDO and EPI models may contribute to the different preload dependency in the time course of contraction in isolated ENDO and EPI cells.

3.1.2. Regional differences in EDFLR and ESFLR

To examine myocardial stiffness and contractility in ENDO and EPI cells, we estimated the slopes of the EDFLR and ESFLR curves (Fig. 7). There were no significant differences in slopes of the EDFLR ($p=0.73$) and in slopes of the ESFLR ($p=0.99$) between the isolated ENDO and EPI cells, specifying their homogeneity in stiffness and contractility. All considered EPI models were the same in terms of EDFLR and showed a small difference of less than 8% against the ENDO model. The EPI models, with the exception of one model with a decreased CaTnC

dissociation rate constant (EPI($\downarrow k_{off}$)), also showed rather small differences that were less than 10% with the ENDO model that reproduced the experimental findings (Fig. 7).

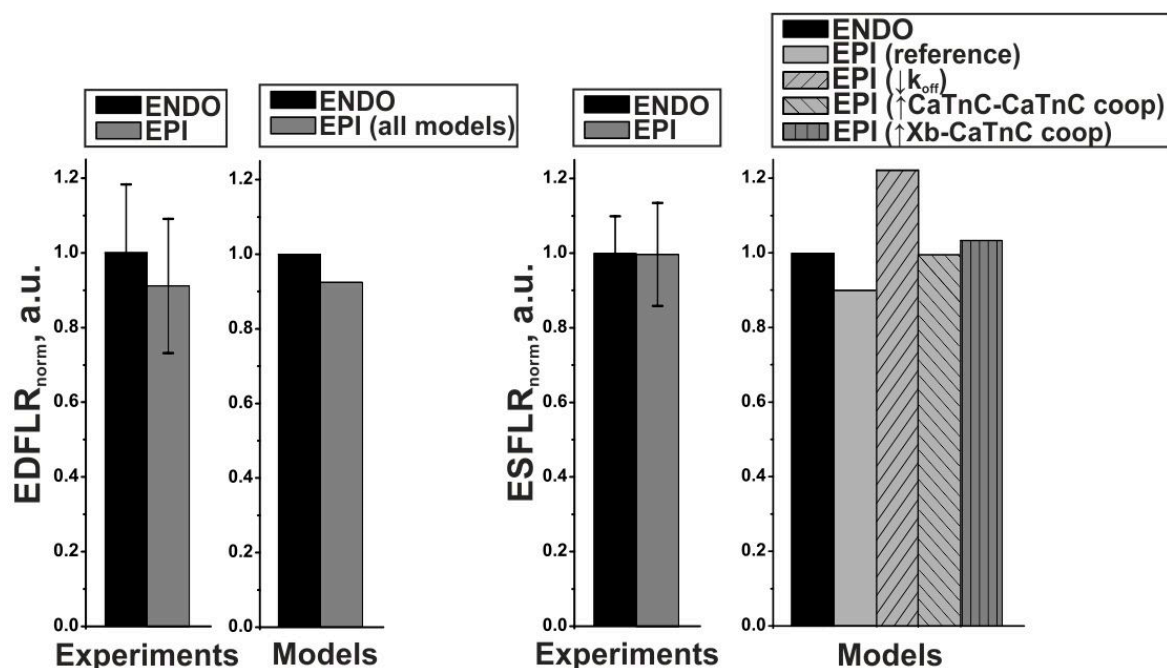


Figure 7. Normalized slope of the EDFLR and ESFLR in mouse ventricular cardiomyocytes in wet experiments (ENDO: $n=25$, EPI: $n=24$) and mathematical models. Values of the EDFLR and ESFLR were normalized by the ENDO values.

3.1.3. Model validation and calcium transient measurements

To examine the transmural differences in excitation–contraction coupling at various preloads and validate our mathematical models we investigated differences in the cellular $[Ca^{2+}]_i$ transient between the ENDO and EPI isolated cells. Figure 8 shows representative $[Ca^{2+}]_i$ transient recorded in ENDO and EPI cardiomyocytes from the same mouse heart.

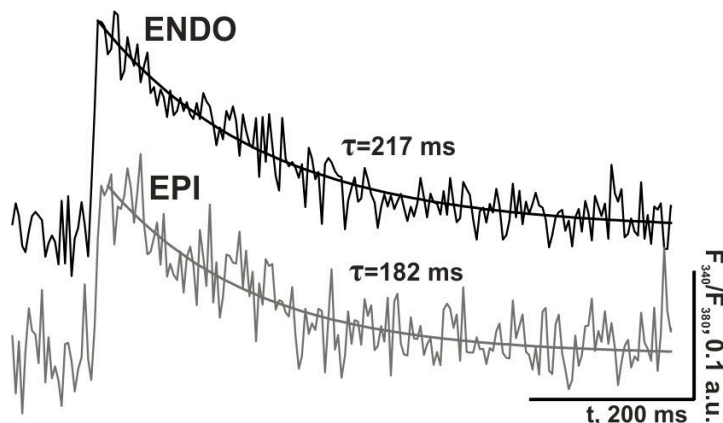


Figure 8. Representative recordings of the $[Ca^{2+}]_i$ transient in ENDO and EPI isolated cardiomyocytes from the same mouse heart. Time constant τ characterizes faster decay of $[Ca^{2+}]_i$ transient in the EPI cell.

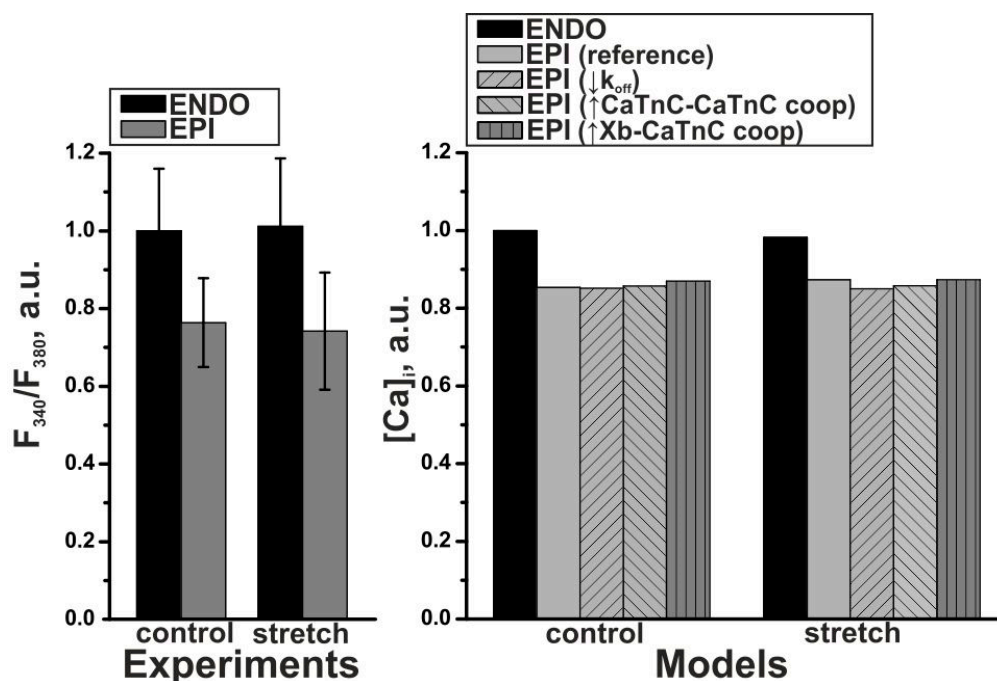


Figure 9. Relative amplitudes of intracellular $[Ca^{2+}]_i$ at various preloads in wet experiments (ENDO: $n=10$, EPI: $n=11$) and mathematical models. Values are normalized by the ENDO values.

While diastolic Ca^{2+} levels were similar ($p=0.63$, data not shown), $[Ca^{2+}]_i$ amplitude in ENDO myocytes tended to be higher compared to EPI myocytes during auxotonic contractions independent of the preload, but the difference was not statistically significant ($p=0.24$, Fig. 9, left panel). We found no stretch effect on the diastolic Ca^{2+} level or $[Ca^{2+}]_i$ amplitude either in isolated ENDO or EPI cells ($p=0.93$, Fig. 9, left panel). Simulation results also showed a lower $[Ca^{2+}]_i$ amplitude in the EPI models, suggesting that this might be a specific feature of the transmural difference in Ca^{2+} dynamics. Stretch did not affect the $[Ca^{2+}]_i$ amplitude in either of the models, which is consistent with the experimental data (Fig. 9, right panel).

The time to peak of $[Ca^{2+}]_i$ transient in ENDO myocytes tended to be greater compared with EPI myocytes, but the difference was not significant (Fig. 10, $p=0.67$). At low preload, the time constant of $[Ca^{2+}]_i$ transient decay (τ) was higher, but not different, in ENDO cells compared with EPI cells (Fig. 10, $p=0.12$). Stretch insignificantly prolonged τ in EPI cells, but not in ENDO cells (interaction between the groups $p=0.49$), which was consistent with the greater preload dependency for T_{max} in the EPI cells (Fig. 9, left panel). All the EPI models produced an increase in τ in the stretched state, while the EPI model, with an increased Xb-CaTnC cooperativity, quantitatively produced the most pronounced response to stretch, which is closer to the experimental data (Fig. 10, right panel, EPI (\uparrow Xb-CaTnC coop)).

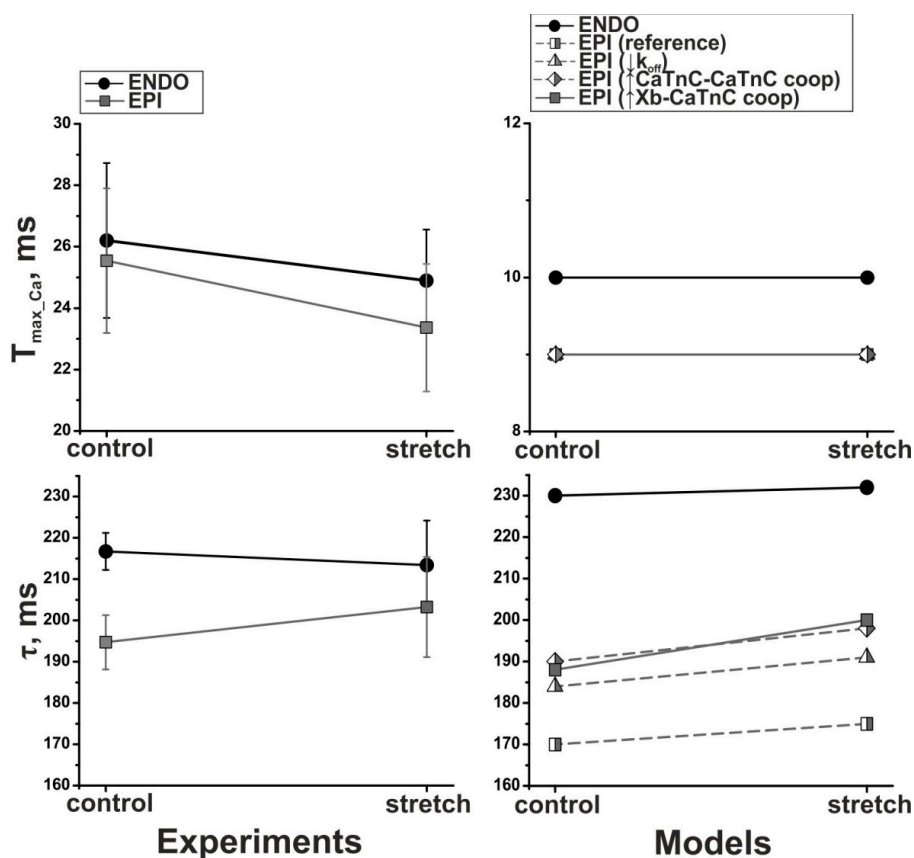


Figure 10. Transmural gradients in time to peak (T_{max_Ca}) and the decay time constant of $[Ca^{2+}]_i$ transient (τ) between ENDO and EPI cells at various preloads in wet experiments (ENDO: n=10, EPI: n=11) and mathematical models.

Despite no significant differences in the amplitudes and time parameters of $[Ca^{2+}]_i$ transient between the isolated cells, there was a trend in our results. We suggest that a decrease in regional differences in $[Ca^{2+}]_i$ under high preload conditions may reflect a different length dependency in the Ca^{2+} activation of myofilaments between the cells, as predicted by our models. Among the EPI models we tested, the only the EPI model with an increased degree of Xb-CaTnC cooperativity was able to produce sufficiently steep length dependency in the decay of Ca^{2+} transient.

3.2. The effects of loading conditions on the transmural gradient in contraction

To compare the time-dependent characteristics of contraction profiles in the isolated ENDO and EPI cells under different loading conditions, we used the instantaneous elastance approach (see Materials and methods). Representative superimposed elastance curves $E(t)$ of heavy loaded (isometric) and unloaded contractions of ENDO and EPI isolated cardiomyocytes at slack SL_0 are shown in Figure 11.

In both cell types, time to the peak of the elastance curve (ET_{max}) was significantly longer ($p < 0.01$, Fig. 12) and time to 50% relaxation (ETR_{50}) was significantly shorter ($p < 0.05$, Fig. 12) under unloaded compared with heavy loaded contractions. Our ENDO and EPI models qualitatively reproduced these experimental results, showing prolongation of ET_{max} and shortening of ETR_{50} with decreasing mechanical load (Fig. 12, right panel).

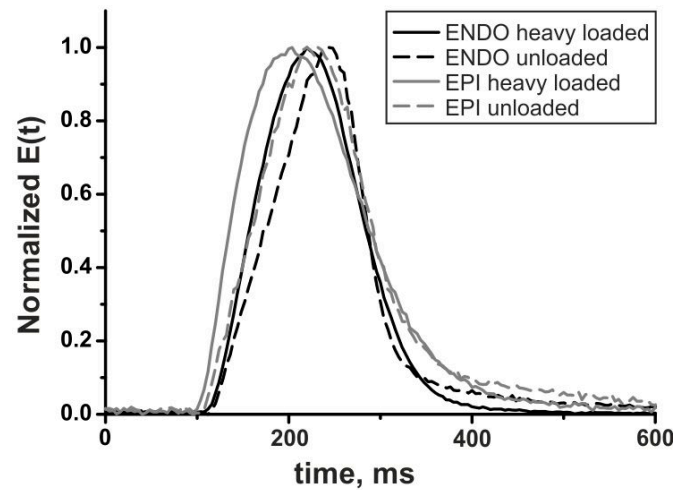


Figure 11. Representative superimposed elastance curves $E(t)$ of heavy loaded (solid lines) and unloaded (dashed lines) contractions of ENDO and EPI isolated cardiomyocytes at slack SL_0 .

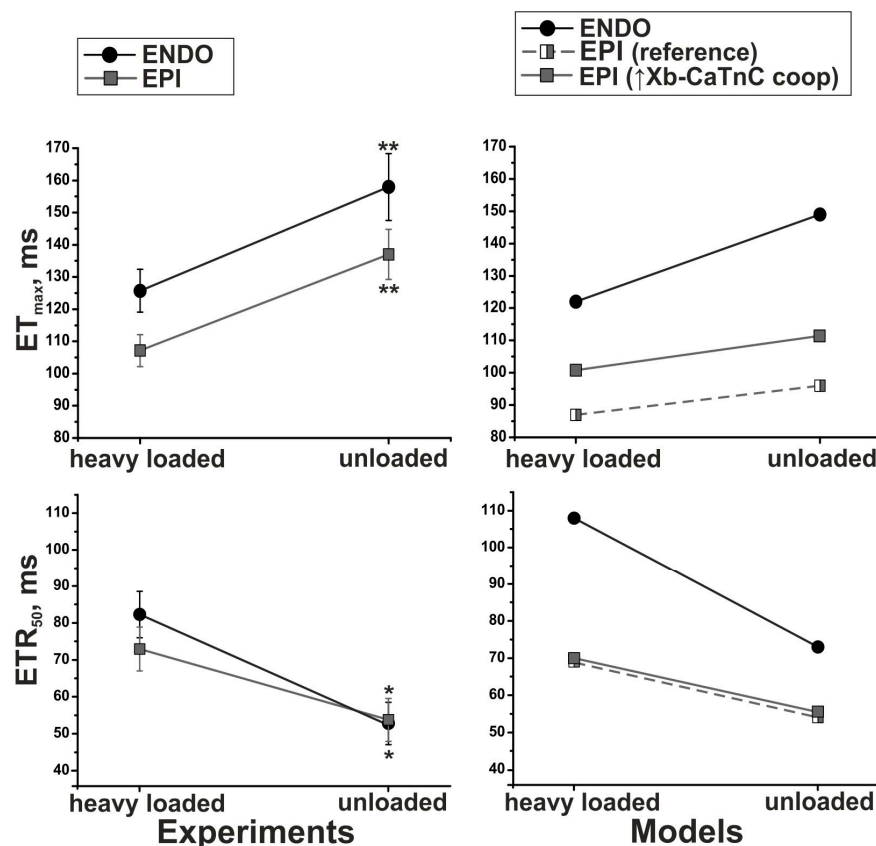


Figure 12. Transmural gradient in the time course of elastance between single ENDO and EPI mouse ventricular cardiomyocytes under unloaded and heavy loaded (isometric)

contraction in wet experiments (ENDO: n=11, EPI: n=9) and mathematical models at slack SL₀. Top panel: time to peak contraction (ET_{max}). Bottom panel: time to 50% relaxation (ETR_{50}). ** Control vs. stretch, $p<0.01$; * Control vs. stretch, $p<0.05$.

ENDO cells demonstrated a longer ET_{max} compared with EPI cells, and this was independent of the load. The relative difference in the mean ET_{max} between ENDO and EPI cells related to the ENDO value was 14% in heavy loaded contractions, and 13% in unloaded contractions, but the differences were not significant ($p=0.07$, Fig. 12). Cellular models qualitatively reproduced these experimental results (Fig. 12, right panel), and the EPI model with an increased Xb-CaTnC cooperativity (EPI(\uparrow Xb-CaTnC coop)) produced closer results to the experimental data among the EPI models, with the relative difference in ET_{max} of 17% under heavy loaded conditions and 26% under unloaded conditions. Transmural differences in ETR_{50} between the ENDO and EPI cells decreased under unloaded contractions (relative difference in the mean TR_{50} between ENDO and EPI cells related to the ENDO value was 11% under heavy loaded, and -2% under unloaded conditions, respectively), but the difference was not significant (interaction between the groups, $p=0.50$). In the ENDO and EPI models, the transmural gradient in ETR_{50} also decreased with a decreasing load, while the differences in ETR_{50} between the cell types were more quantitatively pronounced in the models than in the wet experiments (relative difference in ETR_{50} between ENDO and EPI (\uparrow Xb-CaTnC coop) models was 35% under heavy loaded, and of 23% under unloaded conditions).

We previously discussed the model predictions of the mechanisms underlying the load dependency in both T_{max} and relaxation time in single cardiomyocytes [21, 22]. Briefly, a reduction in the load causes faster shortening, which decreases both instant SL and the end-systolic SL. All these factors reduce the instant [Xb], and thus the affinity of TnC for Ca^{2+} decreases via Xb-CaTnC cooperativity [21, 22]. This results in a prolongation of Ca^{2+} transients that, in turn, delays T_{max} . However, faster dissociation of CaTnC complexes causes a faster decrease in [Xb], resulting in a decrease in the relaxation time constant under low loaded contraction conditions.

As described above (see Mathematical models section), we suggested in the ENDO model that there is a higher *RU end-to-end cooperativity* (cooperative end-to-end interaction between adjacent tropomyosins on the thin filament) than in the EPI model, which resulted in greater amplitude of sarcomere shortening and accordingly active tension of the ENDO cells [18, 20]. Additional simulation experiments showed that because of the higher degree of the *RU end-to-end cooperativity* in the ENDO model, an increase in the instant shortening velocity, and accordingly a decrease in end-systolic SL, were higher in the ENDO model, which results in a

faster decrease in the $[X_b]$ compared to the EPI model as the load decreases. Thus, we reproduced the tendency observed experimentally, where the transmural gradient in TR_{50} decreased under unloaded conditions (Fig. 12).

4. DISCUSSION

In this paper, we presented results on the load dependency in the mechanical properties of isolated ENDO and EPI cardiomyocytes from the mouse LV. The major findings of our work are that that ENDO and EPI cardiomyocytes are different in their mechanical response to a change in load.

4.1. Preload effect upon regional differences in contraction

The effects of preload (or axial stretch) were studied in isolated cells under uncontrolled auxotonic contractions, where cells both shortened and developed force under the mechanical load of the carbon fibers (see Materials and Methods).

We found no significant differences in the slope of the EDFLR and ESFLR curves between the ENDO and EPI cells that were isolated from mouse ventricular LV. Our observations are consistent with findings that were recently reported in cardiomyocytes isolated from the right and left ventricles of the guinea pig [14]. Conversely, Cazorla and co-workers reported on steeper SL-passive tension and SL-active tension relationships in ENDO cardiomyocytes from rat, ferret, and guinea pig ventricles [12, 13]. They used streptomycin, a stretch activated channel blocker at concentrations near 40 μM , to prevent stretch-activated contractions [12, 13]. We have no data on regional differences in the sensitivity of ENDO and EPI cells to streptomycin, but Gannier and co-workers showed that streptomycin may differently affect the stiffness of LV cardiomyocytes, revealing two populations of cells with stronger and weaker responses to streptomycin [23]. Thus, different experimental protocols may explain the discrepancies in the results.

We showed that isolated ENDO cells in mouse LV demonstrate greater time to peak of contraction both at low preload (unstretched state) and high preload (stretched state) (see Fig. 4), which is in agreement with the data addressing transmural features of unloaded ventricular cardiomyocyte shortening in guinea pig [3] and dog [4]. The transmural difference in T_{max} was significant at a low preload, and the difference decreased with an increasing preload because of a steeper preload dependency in T_{max} for the EPI cells (Fig. 4). Consistent with this result, our experimental data showed a tendency for there to be a steeper increase in the decay time constant of the $[\text{Ca}^{2+}]_i$ transient in the stretched state in the EPI cells, which reduced the transmural difference in characteristics of the Ca^{2+} transient between cells with increasing preload (Fig. 10).

Our modeling results reproduce a decrease in the preload-dependent transmural differences between the cells with stretch and suggest that a higher degree of Xb-CaTnC cooperativity in the EPI model may underlie its steeper length dependency in T_{\max} and also via mechano-calcium feedback underlie the steeper length dependency in the decay time constant of the $[Ca^{2+}]_i$ transient, compared with the ENDO model.

We found that an increase in preload does not change $[Ca^{2+}]_i$ amplitude both in ENDO and EPI myocytes. $[Ca^{2+}]_i$ amplitude tended to be higher in ENDO myocytes compared with EPI myocytes (Fig 8), which is consistent with experimental data observed by Kondo and co-workers during unloaded shortening [2].

Measurements of sarcomere length in cardiac preparations confirm that slack SL_0 in the resting Langendorff-perfused heart is longer than in isolated cells [24]. Our findings of a decrease in the preload-dependent transmural differences between the cells suggest that transmural dispersion in cellular shortening may be smaller in the *in vivo* heart compared with our findings in unstretched isolated cells. In the beating heart, the electrical wave of excitation propagates from the subendocardium to the subepicardium [11, 25], so excitation occurs with some time delay between cells that are further apart. This electrical asynchrony causes dynamic changes in the cardiomyocyte lengths, so that the earlier-activated contracting ENDO cardiomyocytes prestretch the passive EPI cells until the excitation wave reaches them. In this case, a steeper length dependency for T_{\max} in EPI cells will help to synchronize regional LV contractions.

However, transmural gradients in the mechanical properties of the myocardial tissue do not disappear completely in the intact heart. Ashikaga and co-workers recently identified the time course of transmural regional strain in the LV anterior wall in normal dog hearts *in vivo* with using biplane cineangiography of implanted transmural markers [10]. They found that there is a regional dispersion of myofiber shortening in the subendocardium and subepicardium despite the lack of significant transmural gradient in the electrical repolarization [10].

The question on the dispersion of the electrical repolarization between ventricular regions in the whole heart is still under consideration. Taggart and co-workers suggested that the transmural gradient in the action potential duration of the cells in the whole heart is often not as pronounced as that in isolated cells, possibly because of the electrotonic coupling of myocytes across the wall [9].

Axial stretch of the single cardiomyocyte was shown to result in a time-independent outward current that decreases the action potential duration (APD) [26]. Other data shows that non-inactivating inward cationic currents may increase APD during stretch [27]. Using our models to make predictions, we suggest that higher cooperativity of interaction between Xbs and

calcium-troponin C complexes in EPI cardiomyocytes cause delayed CaTnC dissociation with increasing preload that results in prolongation of the Ca^{2+} transient. Thus, we may expect that prolongation of the Ca^{2+} transient may also prolong APD in EPI cells, which may contribute to the reduced AP sensitivity to stretch in the EPI cells and may provide a lack of transmural gradient in electrical repolarization in the whole heart where cardiomyocytes are prestretched.

In our mathematical models, we focused on cooperative mechanisms of Ca^{2+} activation of contractile proteins in cardiomyocytes, and the mechanisms of mechano-calcium feedback in cardiomyocytes, while effects of stretch-activated currents on cell behaviour were not examined. Saint and co-workers observed different transmural electrical responses to stretch in rat heart [28] with a more pronounced decrease in the APD in ENDO cells than in EPI cells. Stones and co-workers observed that mRNA levels of TREK-1, a mechanosensitive K^+ channel, were significantly greater in ENDO than in EPI cells, which may underlie greater shortening of AP in stretched ENDO cells and provide greater stretch sensitivity in ENDO cardiomyocytes compared to EPI cells [29]. Thus, we believe that these two phenomena of greater length dependency in T_{\max} in EPI cells, which might cause the prolongation of AP in EPI cells via mechano-electric feedback, and greater mechanosensitive K^+ channel density in ENDO cells, which might provide a decrease of AP in ENDO cardiomyocytes, together or separately may result in a decrease in the transmural gradient in the APD between the cells under stretch conditions. This hypothesis should be addressed in further studies.

4.2. The loading condition effect on regional differences in contraction

To the best of our knowledge, there are no previous studies that address the effects of loading conditions on the transmural difference in the mechanical properties of isolated cells. In this study, we examined, for the first time, specific features of the time course of cellular contraction during isometric (heavy loaded) and unloaded contractions of ENDO and EPI cells.

Effects of loading conditions on the time course of cellular contraction in both ENDO and EPI cell types are consistent with previous studies on single cells that are isolated from the ventricle without taking into account cellular location [15, 16, 30]. Unloaded cellular contractions showed a longer T_{\max} and a shorter TR_{50} compared with heavy loaded conditions, both in wet experiments and in mathematical models. We found that isolated ENDO cells show slower contractions under different loading conditions compared with EPI cells. The regional gradient in the time characteristics of relaxation decreased when the load decreased. Our mathematical models predict that this decrease may be related to the higher degree of the cooperative end-to-end interaction between adjacent tropomyosins on the thin filament in the ENDO cardiomyocytes.

5. LIMITATIONS

In the present study, all recordings were made at a stimulation frequency of 1 Hz at room temperature (22–24°C) to improve the experimental success rate. Temperature may affect transmural differences in the electrical and mechanical function of cells [31]. Therefore, the effect of temperature on the results should be further clarified.

No signal calibration was required because there was no attempt to compare absolute calcium levels.

6. CONCLUSIONS

The main findings of our study are:

- Our experimental and modeling results demonstrate that ENDO and EPI cardiomyocytes are different in their mechanical response to change in preload (axial stretch) with greater length dependency in the time course of EPI cell contraction.
- Simulation results predict that differences in cooperativity of interaction of cross bridges and calcium-troponin C complexes between the ENDO and EPI cardiomyocytes may essentially contribute to the different cellular responses to stretch. This may cause a decrease in transmural dispersion of cellular shortening in the whole heart compared to isolated cells via mechano-calcium-electric feedback.
- Extent of the transmural gradient during contractions is independent of the loading conditions, but there is a tendency for the regional gradient in the time characteristics of relaxation to decrease when the load is decreased.

7. ACKNOWLEDGMENTS

The development of mouse ventricular cardiomyocyte model was supported by the Russian Foundation for Basic Research (#16-31-60015). Wet experiments and simulations were supported by The Russian Science Foundation (#14-35-00005).

8. AUTHOR CONTRIBUTIONS

A.K.: wet experiments, computational simulations, analysis, and interpretation of the results

G.I.: design the wet experiments, analysis, and interpretation of the results

L.K., O.S.: conception of the mathematical models, design, analysis, and interpretation of the results and simulations

K.N.: interpretation of the results

The manuscript was written by A.K., with the assistance of O.S., G.I., and L.K. All authors approved the final version of the manuscript.

References

1. Clark, R.B., et al., *Heterogeneity of action potential waveforms and potassium currents in rat ventricle*. Cardiovascular research, 1993. **27**(10): p. 1795-9.
2. Dilly, K.W., et al., *Mechanisms underlying variations in excitation-contraction coupling across the mouse left ventricular free wall*. The Journal of physiology, 2006. **572**(Pt 1): p. 227-41.
3. Wan, X., S.M. Bryant, and G. Hart, *A topographical study of mechanical and electrical properties of single myocytes isolated from normal guinea-pig ventricular muscle*. Journal of anatomy, 2003. **202**(6): p. 525-36.
4. Cordeiro, J.M., et al., *Transmural heterogeneity of calcium activity and mechanical function in the canine left ventricle*. American journal of physiology. Heart and circulatory physiology, 2004. **286**(4): p. H1471-9.
5. Antzelevitch, C. and J. Fish, *Electrical heterogeneity within the ventricular wall*. Basic research in cardiology, 2001. **96**(6): p. 517-27.
6. Glukhov, A.V., et al., *Transmural dispersion of repolarization in failing and nonfailing human ventricle*. Circulation research, 2010. **106**(5): p. 981-91.
7. Wan, X., et al., *Molecular correlates of repolarization alternans in cardiac myocytes*. Journal of molecular and cellular cardiology, 2005. **39**(3): p. 419-28.
8. Osadchii, O.E., E. Soltysinska, and S.P. Olesen, *Na⁺ channel distribution and electrophysiological heterogeneities in guinea pig ventricular wall*. American journal of physiology. Heart and circulatory physiology, 2011. **300**(3): p. H989-1002.
9. Taggart, P., et al., *Electrotonic cancellation of transmural electrical gradients in the left ventricle in man*. Progress in biophysics and molecular biology, 2003. **82**(1-3): p. 243-54.
10. Ashikaga, H., et al., *Transmural dispersion of myofiber mechanics: implications for electrical heterogeneity in vivo*. Journal of the American College of Cardiology, 2007. **49**(8): p. 909-16.
11. Sengupta, P.P., et al., *Biphasic tissue Doppler waveforms during isovolumic phases are associated with asynchronous deformation of subendocardial and subepicardial layers*. J Appl Physiol (1985), 2005. **99**(3): p. 1104-11.
12. Cazorla, O., J.Y. Le Guennec, and E. White, *Length-tension relationships of sub-epicardial and sub-endocardial single ventricular myocytes from rat and ferret hearts*. Journal of molecular and cellular cardiology, 2000. **32**(5): p. 735-44.
13. Cazorla, O., et al., *Resting tension participates in the modulation of active tension in isolated guinea pig ventricular myocytes*. Journal of molecular and cellular cardiology, 1997. **29**(6): p. 1629-37.
14. Bollensdorff, C., O. Lookin, and P. Kohl, *Assessment of contractility in intact ventricular cardiomyocytes using the dimensionless 'Frank-Starling Gain' index*. Pflugers Archiv : European journal of physiology, 2011. **462**(1): p. 39-48.
15. Iribe, G., et al., *Load dependency in force-length relations in isolated single cardiomyocytes*. Progress in biophysics and molecular biology, 2014. **115**(2-3): p. 103-14.
16. Iribe, G., M. Helmes, and P. Kohl, *Force-length relations in isolated intact cardiomyocytes subjected to dynamic changes in mechanical load*. American journal of physiology. Heart and circulatory physiology, 2007. **292**(3): p. H1487-97.
17. Suga, H., K. Sagawa, and L. Demer, *Determinants of instantaneous pressure in canine left ventricle. Time and volume specification*. Circulation research, 1980. **46**(2): p. 256-63.
18. Khokhlova, A., et al., *Transmural Cellular Heterogeneity in Myocardial Electromechanics*. The Journal of Physiological Sciences, 2016. **Submitted. Preprint: <http://www.preprints.org/manuscript/201611.0015/v1>**.
19. Sulman, T., et al., *Mathematical modeling of mechanically modulated rhythm disturbances in homogeneous and heterogeneous myocardium with attenuated activity of na⁺ -k⁺ pump*. Bulletin of mathematical biology, 2008. **70**(3): p. 910-49.

20. Khokhlova, A., G. Iribe, and O. Solovyova, *Load-dependency in mechanical properties of subepicardial and subendocardial cardiomyocytes* Computing in Cardiology (CinC), 2015. **42**: p. 965-968.
21. Izakov, V., et al., *Cooperative effects due to calcium binding by troponin and their consequences for contraction and relaxation of cardiac muscle under various conditions of mechanical loading*. Circulation research, 1991. **69**(5): p. 1171-84.
22. Katsnelson, L.B., et al., *Influence of viscosity on myocardium mechanical activity: a mathematical model*. J Theor Biol, 2004. **230**(3): p. 385-405.
23. Gannier, F., et al., *Streptomycin reverses a large stretch induced increase in $[Ca^{2+}]_i$ in isolated guinea pig ventricular myocytes*. Cardiovascular research, 1994. **28**(8): p. 1193-1198.
24. Bub, G., et al., *Measurement and analysis of sarcomere length in rat cardiomyocytes in situ and in vitro*. American journal of physiology. Heart and circulatory physiology, 2010. **298**(5): p. H1616-25.
25. Sengupta, P.P., et al., *Left ventricular form and function revisited: applied translational science to cardiovascular ultrasound imaging*. J Am Soc Echocardiogr, 2007. **20**(5): p. 539-51.
26. White, E., et al., *The effects of increasing cell length on auxotonic contractions; membrane potential and intracellular calcium transients in single guinea-pig ventricular myocytes*. Experimental Physiology, 1993. **78**(1): p. 65-78.
27. Zeng, T., G.C. Bett, and F. Sachs, *Stretch-activated whole cell currents in adult rat cardiac myocytes*. American Journal of Physiology-Heart and Circulatory Physiology, 2000. **278**(2): p. H548-H557.
28. Saint, D.A., D. Kelly, and L. Mackenzie, *The contribution of MEF to electrical heterogeneity and arrhythmogenesis*, in *Mechanosensitivity of the Heart*. 2010, Springer. p. 275-300.
29. Stones, R., et al., *Transmural variations in gene expression of stretch-modulated proteins in the rat left ventricle*. Pflugers Archiv : European journal of physiology, 2007. **454**(4): p. 545-9.
30. White, E., M.R. Boyett, and C.H. Orchard, *The effects of mechanical loading and changes of length on single guinea-pig ventricular myocytes*. The Journal of physiology, 1995. **482** (Pt 1): p. 93-107.
31. Chung, C.S. and K.S. Campbell, *Temperature and transmural region influence functional measurements in unloaded left ventricular cardiomyocytes*. Physiological reports, 2013. **1**(6): p. e00158.

